The Variation of Wearable and Implanted Antennas' Performance due to Body Temperature

Sima Noghanian
Wafer LLC & American Public University System
San Diego, CA, USA
sima_noghanian@ieee.org

Josh Stout
PADT Inc.
Tempe, AZ, USA
joshmstout@gmail.com

***Abstract*—Wearable and implanted antennas are of interest for various applications. Most previous studies do not consider the effect of body temperature on the antenna's performance, though tissue dielectric properties are temperature-dependent, and typical human tissue temperature is between 32 °C to 37 °C. In this study, we used the ANSYS HFSS and ANSYS Icepak simulation tool to study the effect of tissue temperature on the performance of a set of antennas placed on the skin layer and implanted inside the muscle tissue. The antennas were designed to work around 1.3 GHz for an ambient temperature of 25 °C. By considering the temperature change from a human body we observed a 9.2%, and 9.0% shift in the center frequency for the implanted and external antennas, respectively.**

I. Introduction

The design of implanted and wearable antennas requires examination of several considerations. These antennas are usually small due to the limitation of the volume and size. They may also be subjected to non-ideal conditions such as bending, stretching, rotation, misalignment, and shape deformation. One condition that needs to be considered is that the human body's temperature varies by location. While the skin might be at 32 °C the deep tissue temperature is around 37 °C. The effects of implanted and wearable antennas for on-body and in-body communication applications have been studied in many papers [1]-[4]. These antennas are designed under the loading effect of high permittivity tissue material. Also, their Specific Absorption Rate (SAR) is often either calculated or measured to comply with the safety requirements. However, the authors often did not consider the changes in the tissue's dielectric properties due to the electromagnetic losses and the corresponding change in temperature. In this paper, we examine the effect of electromagnetic losses on the tissue temperature and how it can change the bandwidth and move the center resonance frequency.

II. The Antennas and The Body Model

We consider a model consisting of two antennas and a layered tissue model. Fig. 1. (a) shows the rough schematic of the external (EX) and implanted (IM) antennas that were considered. The detail of the design with all the dimensions can be found in [1]. The antennas are G-shaped microstrip patch antennas with a shorting pin that controls the resonance frequency. We chose the proposed antenna from [1] with a center frequency of 1.3 GHz. From the wireless power transfer system that is described in [1] we only considered the antennas and removed the coils for simplicity. The EX is built on a substrate with a 106 mm × 106 mm area and the IM is built on a substrate of 39.2 mm × 39.2 mm. The substrate is FR4 covered with layers of silicon for biocompatibility. For details see [1].

Fig. 1 (b) shows the body model and the antennas. The EX is placed on the skin layer, and is assumed to be at a temperature of 32 °C, and the IM is placed at the depth of 4.6 mm from the top side of the muscle layer to the patch layer and assumed to be at 37 °C. The height of the skin layer is 3 mm, and under the skin, there is a 7 mm thick fat layer with a temperature of 35 °C. The complete tissue model is 212 mm × 212 mm × 125 mm.

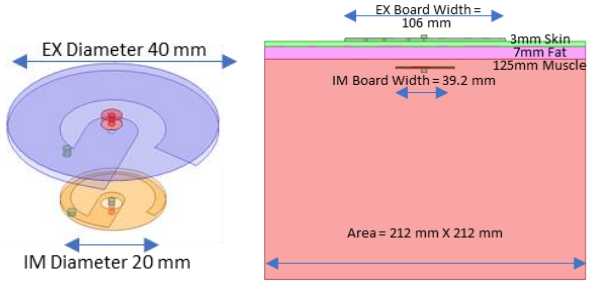

(a) (b)

Fig. 1. (a) Arrangement of the external (EX) and implanted (IM) antennas, (b) the layered tissue body model.

III. The Thermal Model

A. Thermal Dependent Dielectric

In [5] a good review of temperature dependency of the tissue properties of the dielectric properties of various human and animal tissues at different frequencies is provided. This reference states that under 100 °C the dielectric properties dependency is usually estimated by a constant temperature coefficient as:

$$\varepsilon_r = \varepsilon_{ref}(1 + \Delta\varepsilon(T - 37°C)) \quad (1)$$

$$\sigma = \sigma_{ref}(1 + \Delta\boldsymbol{\sigma}(T - 37°C)) \quad (2)$$

where ε_r is the dielectric constant, and σ is the conductivity at the given temperature T. The reference temperature is assumed to be 37 °C. Table I summarizes some of the values given by two studies that are listed in [5]. These are selected due to using a frequency close to our frequency of interest (1.3 GHz) and muscle or liver tissue properties with similar permittivity values as muscle. Based on these values and the tissue properties that are available from various references we chose the tissue properties given in Table II. The thermal variations were

considered by adding the thermal modifiers in ANSYS HFSS 2020R2 material definitions.

TABLE I. SOME EXAMPLES OF MEASURED TEMPERATURE DEPENDENCY OF TISSUES.

Tissue	Freq (MHz)	ε_r	Δε%	σ	Δσ%	Source
Liver, animal	915	48.00	–0.22	0.94	1.29	Brace 2008
Muscle	900	57.00	-0.20	1.00	1.00	Duke 1990

TABLE II. ASSUMED TISSUE AND ANTENNA'S MATERIAL DIELECTRIC AND THERMAL PROPERTIES.

Material	Dielectric Properties					Thermal Properties		
	ε_{ref}	Δε%	σ_{ref}	Δσ%	tanδ	ρ	c	k
Skin	41.405	0	0.8668	0	0.34	1100	3500	0.293
Fat	5.462	0	0.051	0	0.15	910	2500	0.201
Muscle	55.032	-0.2	0.9429	0.01	0.28	1041	3546	0.530
Silicon	11.900	0	0	0	0	2330	712	148
FR4	4.400	0	0	0	0.02	1900	1150	0.294
Copper	1	0	5.8E7	*	0	8933	385	400

*For T>20, 1/(1+0.0039(T-20))

B. Penn's Bioheat Equations

In the calculation of the tissue temperature, the heat transfer equation should be considered. The most used equation for heat transfer in thermal analysis of human tissue is Penn's Bioheat equation [5]:

$$\rho c \frac{\partial T}{\partial t} = \nabla \cdot k \nabla T + \mathbf{J} \cdot \mathbf{E} - \rho_{bl} c_{bl} w_{bl} (T - T_{bl}) + Q_m \quad (3)$$

where ρ is the density (kg/m^3), c is the specific heat (J/kg-C), k is the thermal conductivity (W/m-C), **J** is the current density with the magnitude in (A/m^2), **E** is the electric field intensity with the magnitude in (V/m). T_{bl} is the temperature of blood (°C), ρ_{bl} is the blood density (kg/m^3), c_{bl} is the specific heat of blood (J /kg-K), w_{bl} is the blood perfusion (m^3/m^3-s), and Q_m is the metabolic heat production (W/m^3). The assumed thermal properties of the tissue layers are provided in Table II. In implementing (3) the blue term was calculated by ANSYS Icepak. We assigned zero thermal flux to the surrounding walls, a constant 37 °C to the bottom wall, and natural convection with 25 °C air on the surface of the skin. The red part of (3) was assigned as *EM Loss* and was calculated with a 2-way analysis with ANSYS HFSS. The orange part of (3) was left for future work, as including it alongside the EM loss within Icepak presented a technical challenge.

C. Results

In this study, we started with the HFSS simulations with the assumption that all the material had no thermal information. The dashed lines in Fig. 2 corresponds to the S parameters of the two antennas (EX: port 1 and IM: port 2). We see the change of center frequency for S_{11} from 1.30 GHz to 1.21 GHz, and for S_{22} from 1.30 GHz to 1.18 GHz. In the second part, we attached the model to an Icepak model with a 2-way analysis. We changed the input voltage at each port to (1 V, 3 V, and 10 V) for EX and IM, at a time. Therefore, when EX was excited, IM was receiving, and vice versa. Although these values are extremely high, they were chosen intentionally to see how the temperature inside the tissue changes. Fig. 2 (a) compares the temperature along a line extended from the top of the EX antenna to the bottom of the muscle layer. IM is located around 21 mm along this line. Fig. 2 (b) shows the temperature distribution on the YZ plane for 10 V input at IM. A variation of temperature from 31 °C to 77 °C was observed.

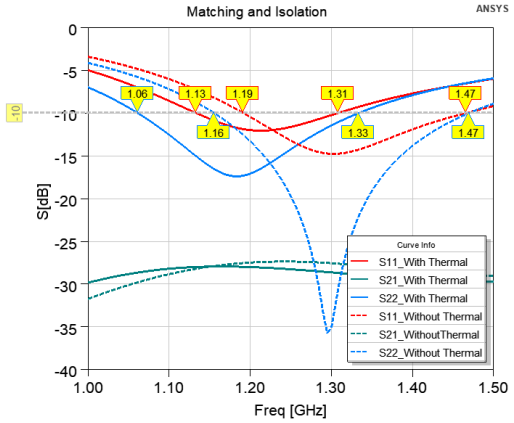

Fig. 2. S parameter comparison with the model that includes thermal information and no thermal variation.

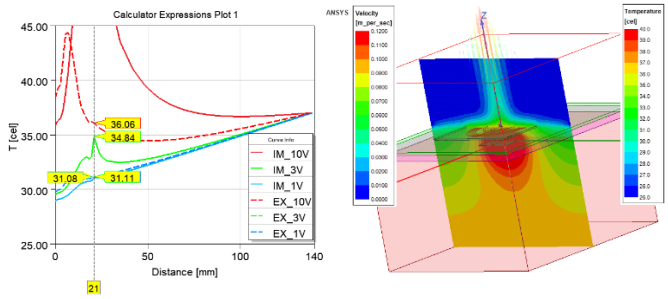

(a) (b)

Fig. 3. (a) Temperature variation at the center of the model moving from the top to the bottom, (b) temperature, and velocity on the YZ axis.

ACKNOWLEDGMENT

We would like to acknowledge Dr. R. Shadid for providing the HFSS files, Dr. S. Gupta, and Dr. A. Sabouni for constructive discussions, PADT Inc. and Wafer LLC for their support.

REFERENCES

[1] R. Shadid, M. Haerinia, S. Roy, and S. Noghanian, "Hybrid inductive power transfer and wireless antenna system for biomedical implanted devices," *Prog. Electromagn. Res. C*, vol. 88, 2018, doi: 10.2528/PIERC18061604.

[2] R. Shadid, M. Haerinia, and S. Noghanian, "Study of rotation and bending effects on a flexible hybrid implanted power transfer and wireless antenna system," *Sensors*, vol. 20, no. 5, pp. 1–10, 2020, doi: 10.3390/s20051368.

[3] A. Alemaryeen and S. Noghanian, "On-body low-profile textile antenna," *IEEE Tran. Antenn. Propag.*, vol. 67, no. 6, pp. 3649–3656, 2019.

[4] A. Alemaryeen and S. Noghanian, "Crumpling effects and specific absorption rates of flexible AMC integrated antennas," *IET Microwaves, Antennas Propag.*, vol. 12, no. 4, 2018, doi: 10.1049/iet-map.2017.0652.

[5] D. J. Schutt and D. Haemmerich, "Effects of variation in perfusion rates and of perfusion models in computational models of radiofrequency tumor ablation," *Med. Phys.*, vol. 35, no. 8, pp. 3462–3470, 2008, doi: 10.1118/1.2948388.